Hindawi
Shock and Vibration
Volume 2021, Article ID 7941242, 8 pages
https://doi.org/10.1155/2021/7941242

Research Article

Experimental Study of the Creep Disturbance Effect and Acoustic Emission Characteristics of Mudstone with Different Moisture Contents

Yongjiang Yu, Pengbo Wang, Shipeng Zhang, and Jingjing Liu

College of Mining Engineering, Liaoning Technical University, Fuxin 123000, China

Correspondence should be addressed to Pengbo Wang; wpb1026754217@163.com

Received 13 September 2021; Revised 13 November 2021; Accepted 25 November 2021; Published 15 December 2021

Academic Editor: Shaofeng Wang

It is important to have a clear understanding of the creep characteristics of water-rich soft rocks under a dynamic load and the evolution of cracks because soft rock roadways in deep mines are very sensitive to disturbances, and instability and damage can easily occur under the impact of disturbances such as mining and blasting. In this study, a self-developed disturbed creep test bench was used to conduct graded loading creep disturbance tests on mudstone specimens with different moisture contents. The results show that an increase in the moisture content leads to a significant increase in the creep failure strain of mudstone, and the accelerated creep rate is greatly accelerated. Moreover, as the moisture content increases, the type of mudstone creep disturbance failure gradually changes from accelerated creep failure to disturbance failure. By analyzing the acoustic emission (AE) characteristics of the mudstone creep disturbance tests, it was found that the increase in the moisture content greatly weakens the AE count and the accumulated energy. In each stage of disturbance, the AE signals jumped, and the stability was restored at the end of the disturbance. As the load increased, the specimen entered the accelerated creep stage, the AE signal increased exponentially, and the internal cracks expanded rapidly until failure occurred. It is of great significance to carry out creep disturbance experiments and to analyze the evolution of the internal cracks in specimens with different moisture contents to maintain the long-term stability of deep soft rocks.

1. Introduction

With the depletion of shallow mineral resources, coal mining is moving to deeper depths [1]. The occurrence environments of deep rock masses are complex. Most of the time, they are under a combined stress state consisting of a static load and dynamic disturbances, and the stress is close to the strength limit. In particular, in the deep, soft rock roadways, the creep deformation is large, the creep rate is fast, and the deformation is in an extremely unstable state. Under the influence of excavation, blasting, and other disturbance actions, local instability is prone to occur, causing the domino effect and ultimately leading to instability and destruction of the roadway [2–6].

The creep characteristics of soft rock cause its failure stress to be far lower than its strength limit, which is a key factor affecting the long-term strength of a rock mass [7]. At present, the theoretical analysis and mechanism research on rock mass creep have been very sufficient [8–14]. In view of the different geological conditions and complex field coupling effects, the component combination method was used to construct the creep model. This method is simple, effective, and highly practical, and it has been used by many scholars [2, 15]. With the development of the theory of damage mechanics, the evolution of cracks during rock mass creep and the mechanism of accelerated creep instability have been gradually revealed. Through computed tomography (CT) and acoustic emission (AE) research, it is possible to accurately observe the initiation and evolution of cracks in a rock specimen and to understand the law of energy release in the different creep stages [16–18]. Heap et al. [19] studied the triaxial brittle creep law of Darley Dale

saturated water sandstone specimens and found that the axial strain rate largely depends on the applied stress difference. By analyzing the location of the AE source, the reliability of the results was confirmed in the context of microstructure analysis. Zhiliang et al. [20] used CT to analyze the damage process and crack evolution characteristics of gray-green mudstone under creep disturbance and to observe the crack expansion in order to describe the different stages of creep. Baud et al. [21] analyzed the creep AE characteristics of a brittle rock mass based on the three stages of creep and found that the AE count and accumulated energy of specimens with similar damage levels under the three-mode behavior of creep were also roughly the same. However, CT and AE equipment are often used to study the creep of a rock mass under constant stress, and there is less research on the creep characteristics of rock masses under dynamic load disturbance. Studies have shown that the creep characteristics of a rock mass under an impact disturbance are significantly different from those without disturbance. Yanfa et al. [22] emphasized the necessity of studying the effects of a dynamic disturbance on the rheological characteristics of rocks and proposed the concept of the rock strength limit neighborhood. Zhu et al. [23] proposed two failure forms that combine a dynamic disturbance and creep stress: accelerated creep failure and dynamic disturbance failure. Through qualitative analysis, the types of creep disturbance failure were classified into two types. Wang et al. [24, 25] carried out creep disturbance experiments with different perturbation amplitudes and frequencies on different soft rock specimens (gneiss and mudstone) using a stepwise loading method, and according to the disturbance creep characteristics, a creep perturbation damage model was established.

In summary, the research on the creep characteristics of rock masses and the law of crack development under a static load has been relatively sufficient. However, whether it is combined with the actual needs of a project or of disaster warning and prediction, the study of the creep characteristics of a rock mass must consider the impact of a dynamic disturbance. Thus, in this study, an independently developed rock rheological disturbance test system was used to conduct graded loading creep disturbance and AE tests on mudstone specimens with different moisture contents. The sound-absorbing cotton was covered with a sound insulation board to avoid the interference of the perturbation on the AE signal. The characteristic AE parameters were used to analyze the creep disturbance process and the crack evolution in mudstone specimens with different moisture contents. The results of this study provide a useful reference for follow-up research on soft rock roadway support in deep engineering and soft rock creep and rupture triggered by disturbances such as excavation and blasting.

2. Mudstone Creep Disturbance Test Scheme

2.1. Test Equipment. The tests were conducted using a self-developed rheological disturbance effect test system and an AE system. The rheological disturbance test system mainly included a self-developed rheological support instrument, a disturbance load loading device, an axial load loading device, and a data acquisition system. The AE system used was the SAEU3H AE system developed by Beijing Shenghua Technology Co., LTD. The test system is shown in Figure 1.

(1) *Axial Loading Device.* Different weights were placed on the weight plate to achieve axial loading. Based on the lever principle, the axial load expansion ratio was 45.

(2) *Disturbance Loading Device.* The vibration motor was placed above the gravity weight, and the vibration of the lever was transmitted to the uniaxial pressure chamber to impose disturbance on the rock sample. The disturbance frequency was 2 Hz. In addition, the noise insulation board was wrapped around the disturbance device, and the inside of the sound insulation board was covered with silencing cotton in order to keep the vibrations from interfering with the AE signal as much as possible.

(3) *Data Acquisition System.* The rheometer was equipped with a KJF25 type pressure and displacement automatic monitoring system with an 89C51 microcontroller as the core, which can be connected to various types of sensors. The monitoring system was composed of an optical coupling interface design and a computer, which performed the functions of data acquisition, information transmission, and remote control operation.

2.2. Specimen Preparation. The interlayer mudstone from the slope of the Anjialing open-pit mine in the Pingshuo China Coal Mine was used in the tests. In order to ensure the comparability of the experimental results, intensive drilling was conducted in the same large piece of rock, and it was processed into 50 mm × 100 mm international standard rock specimens. The propagation velocity and propagation time of the longitudinal wave in the rock specimens were measured using the acoustic wave, and the specimens with large discrete mechanical properties were eliminated to further ensure the uniformity of the specimens' properties and the comparability of the experimental results. In order to study the rheological disturbance effect of the rock under different moisture contents and stress levels, the specimens with at least three different moisture contents were prepared. The dry sample in this test was obtained by drying the rock sample in a baking box. The baking time was 48 h, and the baking temperature was 105 °C. After baking, the sample was weighed, and the moisture content was determined to be 0%. The other samples, with moisture contents of 5% and 10%, were prepared by soaking in water.

2.3. Test Scheme. In the creep disturbance test, the effects of the moisture content and disturbance on the creep characteristics of the mudstone were considered, and the test involving both the moisture content and a dynamic disturbance was carried out using stepwise loading. In order to determine the loading stress level, according to the research results of Yanfa et al. [22], the uniaxial compression

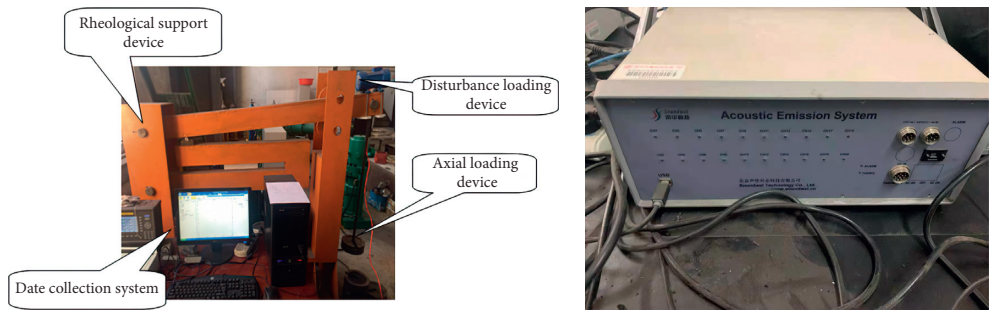

Figure 1: Testing system: (a) rheological testing system; (b) AE system.

experiment was carried out on the mudstone with a moisture content of 10%, and the initial static stress was determined to be 10 MPa. The second stress was 14 MPa, and the third stress was 18 MPa. The disturbance amplitude and frequency of each stage were 0.2 kN and 2 Hz, respectively. In addition, in order to understand the AE characteristics of the rock mass creep disturbance, eight SR150 W sensors were installed around the test specimen (Figure 2).

The test scheme is described in Table 1. According to whether or not there was a disturbance, the tests were divided into two groups. The specific test steps were as follows.

Disturbance Group. Using the hierarchical loading mode, after the axial load was applied in the first stage of the static load, it remained unchanged, and creep deformation was observed. After the creep initially stabilized, the disturbance load was applied for 2 h, and the creep strain was observed. After the creep deformation stabilized (the axial deformation of the rock was less than 0.001 mm within 12 h), the next level of load was applied. After the third stage of static loading and disturbance was applied, the creep strain of the specimen was recorded until it was destroyed. The loading path of each stage is shown in Figure 3. The AE signals of the entire creep process of the specimen were collected.

Undisturbed Group. The static load was applied in the same way as for the disturbed group. The difference was that no dynamic disturbance was applied after the initial creep stabilized in each stage, and the next stage of loading was directly applied after the creep deformation stabilized.

3. Analysis of the Results

3.1. Creep Disturbance of Mudstone with Different Moisture Contents. According to the experimental results, the creep curves of the specimens with moisture contents of 0%, 5%, and 10% in the disturbed and undisturbed states are drawn (Figure 4). The effect of the disturbance on the creep of the mudstone specimens with different moisture contents was analyzed.

By analyzing the creep curves of the mudstone specimens with different moisture contents without disturbance (Figure 4), it was found that the strain of the accelerated creep failure of the mudstone with a moisture content of 0%

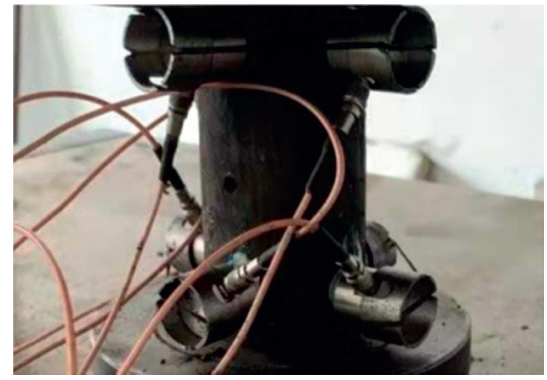

Figure 2: Sensor placement.

Table 1: Test scheme.

Specimen number	Axial compression (MPa)	Moisture content (%)	Dynamic disturbance
D-1	10–18	0	Applied
D-2	10–18	0	—
M-1	10–18	5	Applied
M-2	10–18	5	—
S-1	10–18	10	Applied
S-2	10–18	10	—

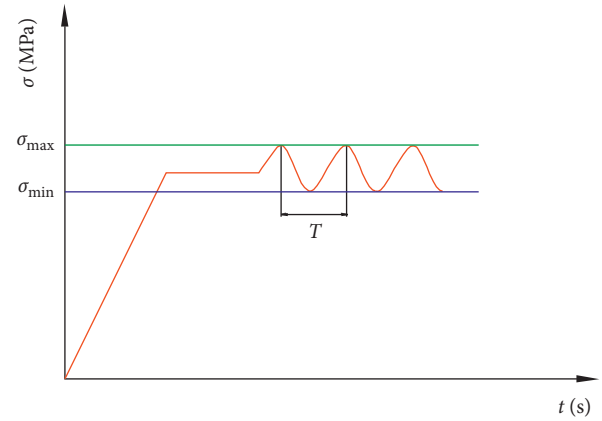

Figure 3: Loading path.

was 27.9×10^{-3}. Accelerated creep failure occurred for the specimens with a moisture content of 5%, and the failure strain was 36.2×10^{-3}. The strain of the specimen with a

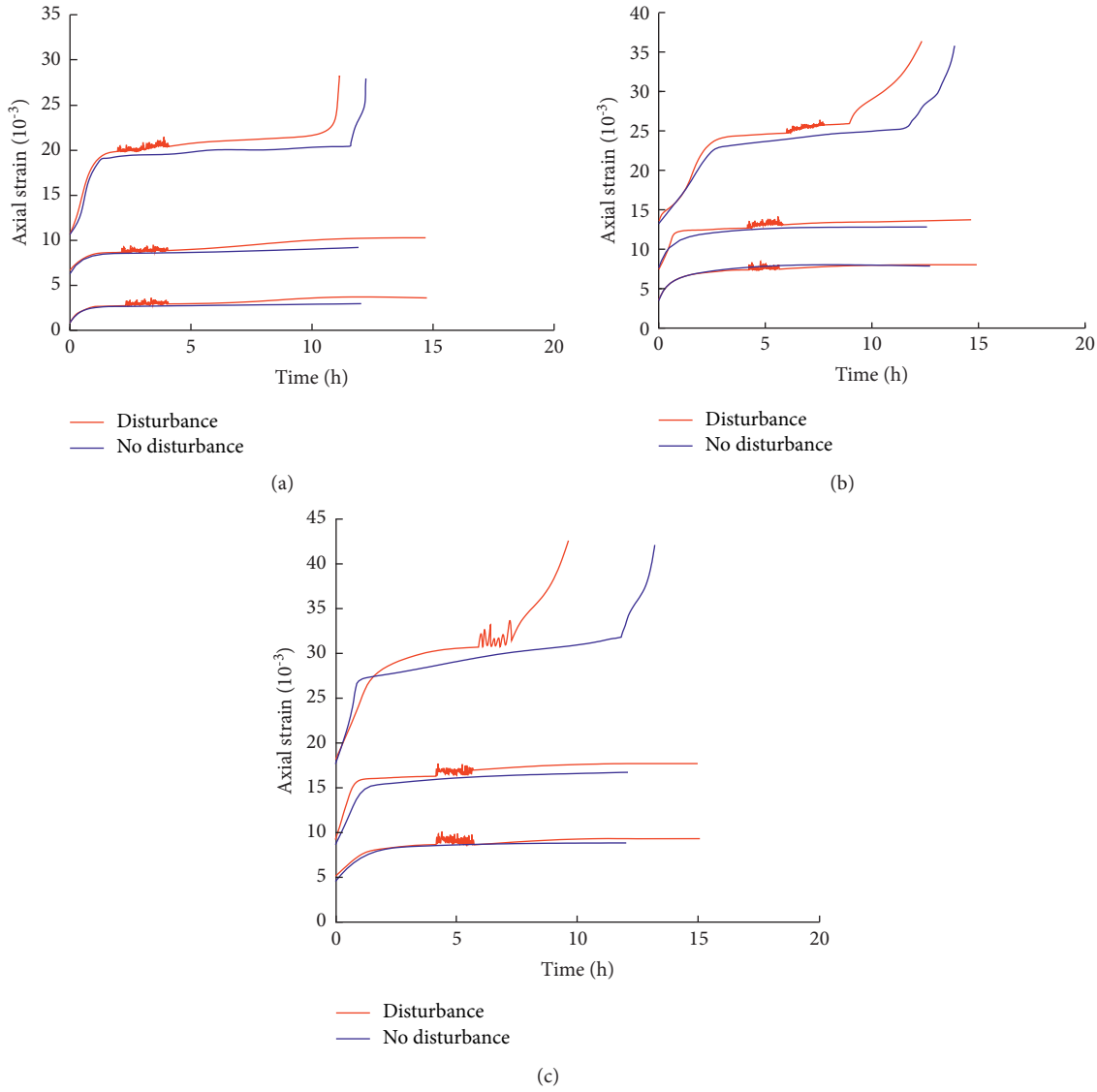

Figure 4: Creep disturbance curves for the mudstone specimens with different moisture contents: (a) $\omega = 0\%$; (b) $\omega = 5\%$; (c) $\omega = 10\%$.

moisture content of 10% was 42.7×10^{-3}. As the moisture content increased, the accelerated creep failure strain of the mudstone increased significantly. The creep rates of the undisturbed specimens with different moisture contents are shown in Figure 5. The static loads in Figures 5(a) and 5(b) are 10 MPa and 14 MPa, respectively, and no accelerated creep occurred in the specimens. The creep rate decreased rapidly from the initial high level and converged to the horizontal axis, and the creep rate of the specimen with a high moisture content was higher than that of the specimen with a low moisture content. This is because the increase in the moisture content changed the mudstone's mineral composition, volume expansion, and microstructure; and the increase in the creep effect led to acceleration of the creep rate. Figure 5(c) shows that for the $\sigma = 18$ MPa case, the mudstone creep rate curve is a horseshoe shape; that is, it initially decreases rapidly and then becomes stable. As the specimen entered the accelerated creep stage, the creep rate increased rapidly, and the rate in the accelerated creep stage was greater than that in the decayed creep stage.

By comparing the creep disturbance curves of the mudstone specimens with different moisture contents (Figure 4) under $\sigma = 18$ MPa, it was found that the mudstone specimens with moisture contents of 0% and 5% first exhibited attenuation and constant creep stages. After the creep deformation became stable, the disturbance was applied, and the creep curves fluctuated accordingly and quickly flattened out after the disturbance ended. With the gradual increase in the creep deformation, the specimens underwent accelerated creep until the creep changed to destruction. When the specimen with a moisture content of 10% was disturbed after the creep deformation became stable, the mudstone creep curve fluctuated sharply, and the creep deformation increased sharply compared with the specimens with moisture contents of 0% and 5%. When the disturbance lasted for 96 min, the creep strain increased suddenly and disturbance failure occurred. The failure of the specimen was caused by the combined action of the

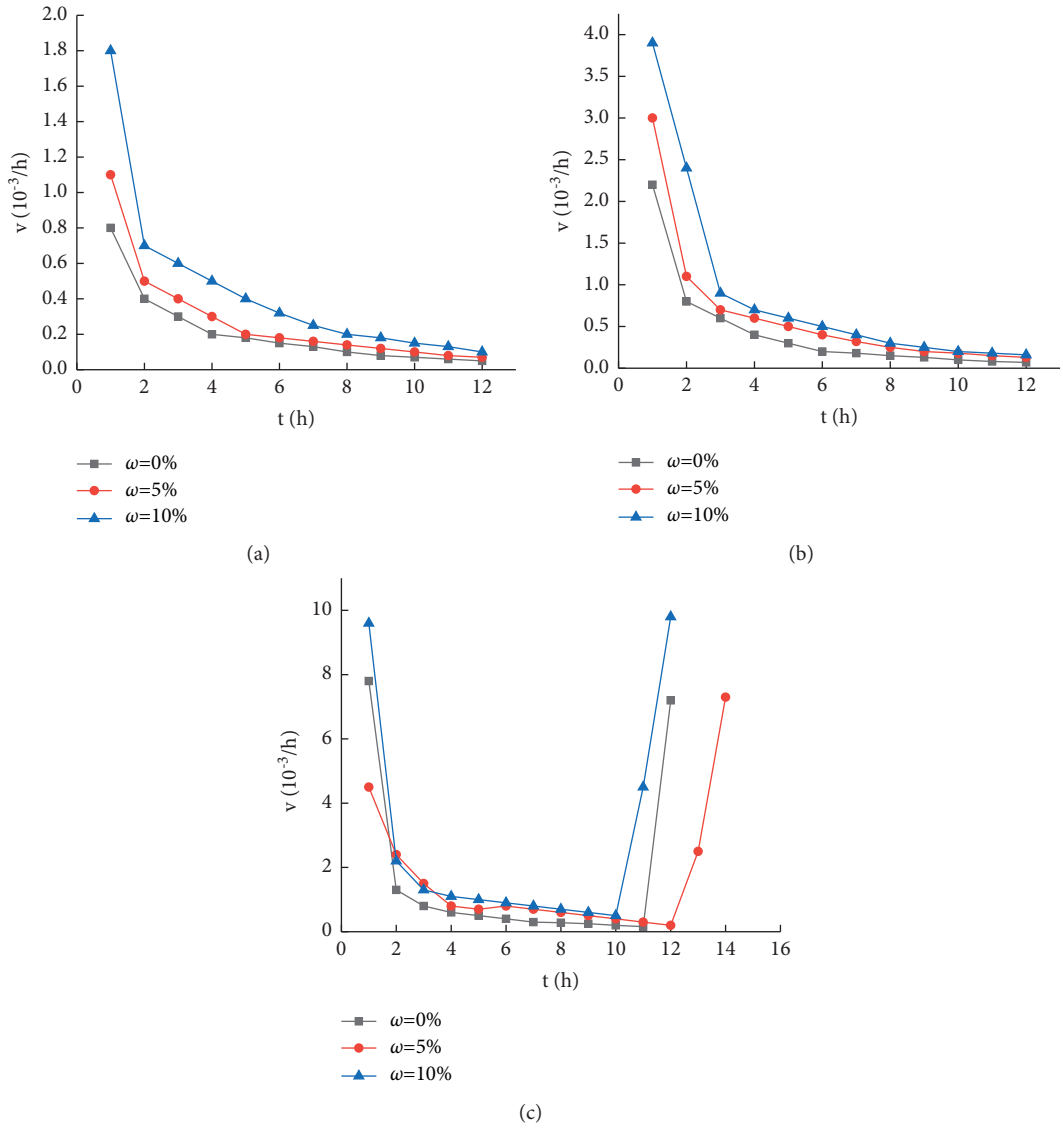

Figure 5: Creep velocity curves for the mudstone specimens with different moisture contents: (a) $\sigma = 10$ MPa; (b) $\sigma = 14$ MPa; (c) $\sigma = 18$ MPa.

accelerated creep and the dynamic disturbance. The failure of the mudstone specimens with moisture contents of 0% and 5% under $\sigma = 18$ MPa was caused by accelerated creep, and the failure mode was accelerated creep failure. The failure of the mudstone specimen with a moisture content of 10% under $\sigma = 18$ MPa was caused by accelerated creep and dynamic disturbance, and the failure mode was disturbance failure.

The influence of the disturbance on the creep strain of the specimens varied dynamically according to the different creep stress levels. When the creep stress was low ($\sigma = 10$ MPa) (Figure 4(c)), the creep strain of the disturbed specimen was 9.2×10^{-3} and that of the undisturbed specimen was 8.9×10^{-3}. The disturbance had little effect on the creep strain. When the creep stress was $\sigma = 14$ MPa, the creep strain of the disturbed specimen was 18.6×10^{-3} and that of the undisturbed specimen was 15.7×10^{-3}. The disturbance effect was more obvious. When $\sigma = 18$ MPa, the disturbance caused the mudstone creep curve to fluctuate significantly, and the disturbance effect was extremely obvious; however, as the specimen entered the accelerated creep stage, it failed. The creep failure strain of the disturbed specimen was 43.2×10^{-3}, and the failure strain of the undisturbed specimen was 42.7×10^{-3}. The creep strain increase factor was 1.02, indicating that the disturbance had no significant effect on the final creep failure strain.

3.2. AE Characteristics of Creep Disturbance. The AE system was used to monitor the entire process of the creep disturbance of the mudstone, to analyze the internal damage and fracture evolution, and to better understand the failure mechanism of the creep disturbance of the mudstone. The creep disturbance of the mudstone specimens with different moisture contents was analyzed using AE characterization parameters, including the AE count and absolute energy. The AE count can reflect the internal brittle fracture damage of the specimen during the process of mudstone creep disturbance better, and the cumulative absolute energy can be used to analyze the creep disturbance characteristics of

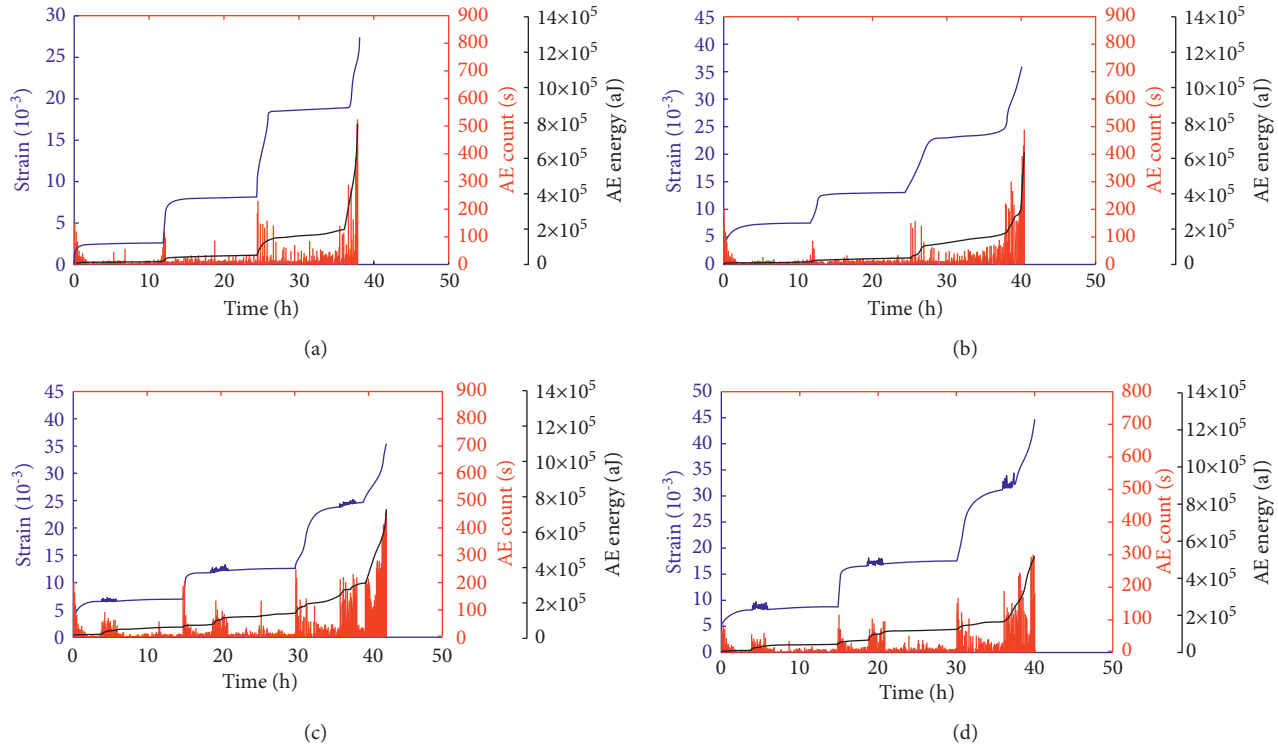

FIGURE 6: Creep and acoustic emission characteristics of the specimens with different moisture contents under disturbed and undisturbed conditions: (a) 0% moisture content, undisturbed; (b) 5% moisture content, undisturbed; (c) 5% moisture content, disturbed; (d) 10% moisture content, disturbed.

the mudstone and the energy released during the creep disturbance to cataclastic transition. Figure 6 shows the creep curve and AE characteristics of the specimens with different moisture contents in the disturbed and undisturbed states.

The AE count and cumulative AE energy statistics of the mudstone specimens under each stress level are presented in Table 2.

The AE characteristics of the specimens with different moisture contents are shown in Figures 6(a) and 6(b). The peak AE count of the specimen with a moisture content of 0% was 522 counts/s, and the accumulated energy of the AE was 7.98×10^5 aJ, while the peak AE count of the specimen with a moisture content of 5% was 482 counts/s, and the accumulated energy was 6.45×10^5 aJ. When the moisture content of the mudstone increased from 0% to 5%, the peak value of the AE ring count decreased by 7.66%, and the energy decreased by 19.2%. Because the increase in moisture reduced the internal particle cohesion of the mudstone, the internal structure was looser, the development of pores and fissures was more difficult, and the instantaneous release of energy upon failure was small, which greatly decreased the AE count and accumulated energy.

In order to understand the influence of the disturbance on the creep AE of the specimens, comparative analysis of Figures 6(b) and 66(c) is conducted. The AE count of the undisturbed mudstone sample with a moisture content of 5% increased instantly when the first static load was applied. As the specimen entered the stable creep stage, the AE count remained stable in a lower range. This situation was repeated under the second- and third-level static loads. When the specimen entered the accelerated creep stage, the count increased sharply, reaching 482 counts/s before the specimen was destroyed, and the cumulative AE energy of the specimen was 6.45×10^5 aJ. The AE counts of the 5% moisture content disturbance specimen increased instantaneously after each level of disturbance was applied; the final AE cumulative energy was 7.26×10^5 aJ; and the cumulative energy increase coefficient of the disturbance to the AE was only 1.13. By comparing the cumulative AE energies of the 5% moisture content mudstone specimens with and without disturbance, it was found that the internal stress balance of the specimen was destroyed after the disturbance was applied, and crack propagation released part of the elastic energy in advance, leading to less elastic energy being released in the accelerated creep stage, whereas undisturbed specimens released a large amount of elastic energy in the accelerated creep stage; so, the cumulative AE energy difference between the disturbed and undisturbed states was not large.

Based on the AE count characteristics of the mudstone creep disturbance, the internal damage and crack evolution of the specimen were analyzed. Directly after the application of the static load in each stage, the AE counts were relatively active. In this stage, the mudstone stress was constantly adjusted, the internal particles were constantly moving, and the primary cracks and pores were compressed and compacted. In the stable creep stage, the AE count entered the

Table 2: Characteristic AE parameters of the creep disturbance of the mudstone specimens with different moisture contents.

Specimen number	Average AE count per level (s)			AE count (s)	Cumulative AE energy (aJ)
	$\sigma = 10$ MPa	$\sigma = 14$ MPa	$\sigma = 18$ MPa		
D-2	32	54	77	522	7.98×10^5
M-2	29	48	70	482	6.45×10^5
M-1	101	148	272	460	7.26×10^5
S-1	78	104	268	312	5.23×10^5

stable lower region, the mudstone stress was balanced, and the damage developed slowly. In the disturbance stage, the AE counts increased greatly, but they returned to a lower level after the disturbance. In this stage, the disturbance broke the stress balance of the specimen, and the internal microcracks continued to expand, but it was not sufficient to cause macroscopic failure of the specimen. As the specimen entered the accelerated creep stage, the AE signal increased exponentially, the specimen's damage reached the threshold, the stress balance was destroyed, and the internal cracks expanded and penetrated the specimen, resulting in a large number of dislocation extrusions, and finally failure occurred.

4. Conclusions

(1) As the moisture content increased, the creep rate and accelerated creep failure strain of the mudstone both increased significantly. In addition, the higher moisture content made the mudstone creep more sensitive to disturbance.

(2) As the moisture content of the mudstone specimen increased from 0% to 5%, the peak value of the AE count decreased by 7.66% and the energy decreased by 19.2%. When the moisture content was increased, the adhesion force of the particles in the mudstone specimen was reduced, the internal structure was loosened, the development of pores and cracks was difficult, and the energy released at the moment of failure was small, which greatly decreased the AE count and the accumulated energy.

(3) The crack propagation released part of the elastic energy in advance, resulting in less elastic energy being released from the disturbed specimens in the accelerated creep stage, whereas the undisturbed specimen released a lot of elastic energy in the accelerated creep stage, and therefore the cumulative energy of the AE in the disturbed and undisturbed states exhibited little difference.

(4) Directly after the static load was applied in each stage, the AE count was more active. In this stage, the internal particles of the mudstone specimen were constantly moving, and the primary cracks and pores were compacted. In the stable creep stage, the AE signal entered a stable lower range, and the damage to the mudstone specimen slowly developed. The AE count increased significantly during the perturbation stage, but it returned to a lower level when the perturbation ended. In this stage, the perturbation broke the stress balance of the specimen, and the internal microcracks continued to expand, but it was not sufficient to cause macroscopic damage to the specimen. As the specimen entered the accelerated creep stage, the AE count increased exponentially, the damage to the specimen reached the threshold, and the internal cracks became connected, resulting in a large number of staggered extrusions and finally failure.

Data Availability

The data used to support the findings of this study are included within the article.

Conflicts of Interest

The authors declare that they have no conflicts of interest.

Acknowledgments

This research was supported by the discipline innovation team of Liaoning Technical University (LNTU20TD-05).

References

[1] X. B. Li and F. Q. Gong, "Research progress and prospect of deep mining rock mechanics based on coupled static-dynamic loading testing," *Journal of China Coal Society*, vol. 46, no. 3, pp. 846–866, 2021.

[2] D. F. Malan, "Time-dependent behaviour of deep level tabular excavations in hard rock," *Rock Mechanics and Rock Engineering*, vol. 32, no. 2, pp. 123–155, 1999.

[3] D. Ma, Y. Zhou, and C. Liu, "Creep behavior and acoustic emission characteristics of coal samples with different moisture content," *Acta Geodynamica et Geomaterialia*, vol. 15, no. 4, pp. 405–412, 2018.

[4] D. Song, E. Wang, N. Li, H. Li, and W. Xu, "Test study of the perturbation effect of coal measures rocks damage failure," *Journal of China University of Mining & Technology*, vol. 40, no. 4, pp. 530–535, 2011.

[5] J. Liu, H. Jing, B. Meng, L. Wang, X. Zhang, and J. Yang, "Research on the effect of moisture content on the creep behavior of weakly cemented soft rock and its fractional-order model," *Rock and Soil Mechanics*, vol. 41, no. 8, pp. 2609–2618, 2020.

[6] X. Cai, C. Cheng, Z. Zhou, H. Konietzky, Z. Song, and S. Wang, "Rock mass watering for rock-burst prevention: some thoughts on the mechanisms deduced from laboratory results," *Bulletin of Engineering Geology and the Environment*, vol. 80, no. 11, pp. 8725–8743, 2021.

[7] J. L. Urai, C. J. Spiers, H. J. Zwart, and G. S. Lister, "Weakening of rock salt by water during long-term creep," *Nature*, vol. 324, no. 6097, pp. 554–557, 1986.

[8] H. Molladavoodi and A. Mortazavi, "A damage-based numerical analysis of brittle rocks failure mechanism," *Finite Elements in Analysis and Design*, vol. 47, no. 9, pp. 991–1003, 2011.

[9] N. Brantut, P. Baud, M. J. Heap, and P. G. Meredith, "Micromechanics of brittle creep in rocks," *Journal of Geophysical Research: Solid Earth*, vol. 117, no. B8, 2012.

[10] A. Nicolas, J. Fortin, J. B. Regnet et al., "Brittle and semibrittle creep of Tavel limestone deformed at room temperature," *Journal of Geophysical Research: Solid Earth*, vol. 122, no. 6, pp. 4436–4459, 2017.

[11] P. Baud, A. Schubnel, M. Heap, and A. Rolland, "Inelastic compaction in high-porosity limestone monitored using acoustic emissions," *Journal of Geophysical Research: Solid Earth*, vol. 122, no. 12, pp. 9989–10010, 2017.

[12] H. F. Deng, M. L. Zhou, J. L. Li, X. S. Sun, and Y. L. Huang, "Creep degradation mechanism by water-rock interaction in the red-layer soft rock," *Arabian Journal of Geosciences*, vol. 9, no. 12, pp. 1–12, 2016.

[13] S. Mighani, Y. Bernabé, A. Boulenouar, U. Mok, and B. Evans, "Creep deformation in Vaca Muerta shale from nano-indentation to triaxial experiments," *Journal of Geophysical Research: Solid Earth*, vol. 124, no. 8, pp. 7842–7868, 2019.

[14] M. Gasc-Barbier, S. Chanchole, and P. Bérest, "Creep behavior of Bure clayey rock," *Applied Clay Science*, vol. 26, no. 1-4, pp. 449–458, 2004.

[15] N. P. Ju, H. F. Huang, D. Zheng, X. Zhou, and C. Q. Zhang, "Improved Burgers model for creep characteristics of red bed mudstone considering water content," *Rock and Soil Mechanics*, vol. 37, no. 2, pp. 67–74, 2016.

[16] K. Du, X. Li, S. Wang, M. Tao, G. Li, and S. Wang, "Compression-shear failure properties and acoustic emission (AE) characteristics of rocks in variable angle shear and direct shear tests," *Measurement*, vol. 183, Article ID 109814, 2021.

[17] K. Du, X. Li, M. Tao, and S. Wang, "Experimental study on acoustic emission (AE) characteristics and crack classification during rock fracture in several basic lab tests," *International Journal of Rock Mechanics and Mining Sciences*, vol. 133, Article ID 104411, 2020.

[18] D. Lockner, "The role of acoustic emission in the study of rock fracture," *International Journal of Rock Mechanics and Mining Science & Geomechanics Abstracts*, vol. 30, no. 7, pp. 883–899, 2021.

[19] M. J. Heap, P. Baud, P. G. Meredith, A. F. Bell, and I. G. Main, "Time-dependent brittle creep in Darley Dale sandstone," *Journal of Geophysical Research: Solid Earth*, vol. 114, no. B7, 2009.

[20] Z. Fu, H. Guo, and Y. Gao, "Creep damage characteristics of soft rock under disturbance loads," *Journal of China University of Geosciences*, vol. 117, no. 3, pp. 292–297, 2008.

[21] P. Baud and P. G. Meredith, "Damage accumulation during triaxial creep of darley dale sandstone from pore volumometry and acoustic emission," *International Journal of Rock Mechanics and Mining Sciences*, vol. 34, pp. 3-4, 1997.

[22] Y. Gao, H. Xiao, B. Wang, and Y. Zhang, "A rheological test of sandstone with perturbation effect and its constitutive relationship study," *Chinese Journal of Rock Mechanics and Engineering*, vol. 27, no. 1, pp. 3180–3185, 2008.

[23] W. Zhu, S. Li, S. Li, and L. Niu, "Influence of dynamic disturbance on the creep of sandstone: an experimental study," *Rock Mechanics and Rock Engineering*, vol. 52, no. 1, pp. 1023–1039, 2019.

[24] J. Wang, Q Sun, B. Liang, P. Yang, and Q. Yu, "Mudstone creep experiment and nonlinear damage model study under cyclic disturbance load," *Scientific Reports*, vol. 10, no. 1, pp. 1–10, 2020.

[25] J. Wang, B. Liang, and P. Yang, "Creep experiment and nonlinear disturbance creep model of gneiss under dynamic and static loads," *Journal of China Coal Society*, vol. 44, no. 1, pp. 192–198, 2019.